ACCEPTED MANUSCRIPT

Observation of bond enthalpy dependence of insulating character in rare earth substituted BiFeO3

Observation of bond enthalpy dependence of insulating character in rare earth substituted BiFeO$_3$

T. Durga Rao[1, 2, a)], Saket Asthana[1, b)]

[1]*Advanced Functional Materials Laboratory, Indian Institute of Technology Hyderabad, Telangana-502285, India*
[2]*Department of Physics, Institute of Science, GITAM University, Visakhapatnam, Andhra Pradesh-530045, India*

Corresponding authors: durgarao.tadisetti@gitam.edu [a], asthanas@iith.ac.in [b]

Abstract

The temperature dependence of impedance and dielectric properties of BiFeO$_3$ (BFO) and Bi$_{0.90}$R$_{0.10}$FeO$_3$ (where R = La, Nd, Eu, Gd and Ho) compounds were investigated. The detailed impedance studies indicated that substitution of rare earth elements significantly enhanced the insulating character of BFO. The enhancement of insulating character was attributed to the improved grain and grain boundary resistances in the substituted compounds. A systematic variation of grain and grain boundary resistances, relaxation times and activation energies in Bi$_{0.90}$R$_{0.10}$FeO$_3$ compounds was observed and explained based on the concept of bond enthalpy. The dielectric anomaly in BFO around the temperature 493 K got suppressed with the substitution of rare earth elements and the amount of suppression was discussed on the strength of R-O bond enthalpies. The impedance, *ac* conductivity and dielectric data corroborated with the idea that the insulating character in Bi$_{0.90}$R$_{0.10}$FeO$_3$ compounds was strongly dependent on the strength of bond enthalpies of R-O bonds.

Introduction

The prominent room temperature magneto-electric properties of BiFeO$_3$ (BFO) has made it as a potential candidate for technological applications such as spintronics, sensors, and data storage devices [1, 2]. BFO is a rhombohedrally distorted perovskite with *R3c* space group. It shows *G*-type antiferromagnetic ordering below Néel temperature (T_N =) 643 K and ferroelectricity below Curie temperature (T_C =) 1103 K [3]. It is a lead-free ferroelectric material which exhibits very high electric polarization (~ 100 μC/cm^2 in thin film form) [4]. In contrast to thin films, bulk BFO ceramics exhibit weak ferroelectric properties due to the presence of large leakage current and impurity phases such as Bi$_2$Fe$_4$O$_9$ and Bi$_{25}$FeO$_{40}$ which limits the potential of BFO in device applications [5]. The presence of coexistence of mixed valence states of Fe (i.e., Fe^{2+} and Fe^{3+}) and oxygen vacancies are the prime contributors to the leakage currents [6]. Several groups have succeeded in improving the multiferroic properties, suppressing the secondary phases

and reducing the leakage currents by substituting rare earth elements at *A*-site [7-12]. There are a few reports addressing the influence of substitution of focused rare earth element at various substitution levels on the insulating character of BFO [13-19]. The potential of the rare earth element to tune the insulating character cannot be compared as different groups follow different synthesis strategies. In order to compare their potential, the level of substitution and synthesis conditions should be the same. It is observed that several reports have claimed that the substitution of 10 mol % of rare earth elements at *A*-site enhances the electrical properties (i.e., reduces leakage currents) and helps in forming phase pure BFO [16, 20, 21]. Therefore, the systematic study of substitution of various rare earth elements at fixed 10 mol % at *A*-site on the electrical properties (i.e., on grain and grain boundary resistances, *ac* conductivity etc) will probably be helpful to streamline some of the issues related to possible applications. Hence, in this work, rare earth lanthanides La, Nd, Eu, Gd and Ho are chosen to substitute at *A*-site of BFO and their impedance, *ac* conductivity and dielectric properties are analyzed. This study will be of great interest to the research community to understand the potential rare earth substituent in tuning the insulating character of BFO.

Experimental

Polycrystalline BFO and $Bi_{0.90}R_{0.10}FeO_3$ (BRFO10) [R = La (BLFO10), Nd (BNFO10), Eu (BEFO10), Gd (BGFO10) and Ho (BHFO10)] compounds were synthesized by conventional solid-state reaction technique using a high purity oxides Bi_2O_3, Fe_2O_3, La_2O_3, Nd_2O_3, Eu_2O_3, Gd_2O_3 and Ho_2O_3 as starting materials. The detailed experimental analysis can be found elsewhere [22]. Phase analysis of the compounds was confirmed by using X-ray diffractometer (Panalytical X'pert Pro) with Cu K_α radiation ($\lambda = 1.5406$ Å). The temperature and frequency dependent impedance and dielectric measurements were performed using a precision impedance analyzer (Wayne Kerr 6500B) on a pellet with silver coating on both the surfaces.

Results and discussion

X-ray diffraction studies

X-ray diffraction (XRD) patterns of BFO and BRFO10 compounds are shown in figure 1. A trace amount of impurity phases such as $Bi_{25}FeO_{40}$ and $Bi_2Fe_4O_9$ (which are designated as ♦ and ∗ respectively) are observed. These phases are suppressed partially with the substitution of Eu,

Gd and Ho whereas La and Nd substitutions form phase pure BFO. Rietveld refinement indicates that BFO, BLFO10 and BNFO10 compounds are stabilized in rhombohedral structure with *R3c* space. However, nominal percentages of orthorhombic phases are observed in BEFO10, BHFO10 and BGFO10 compounds along with *R3c* phase.
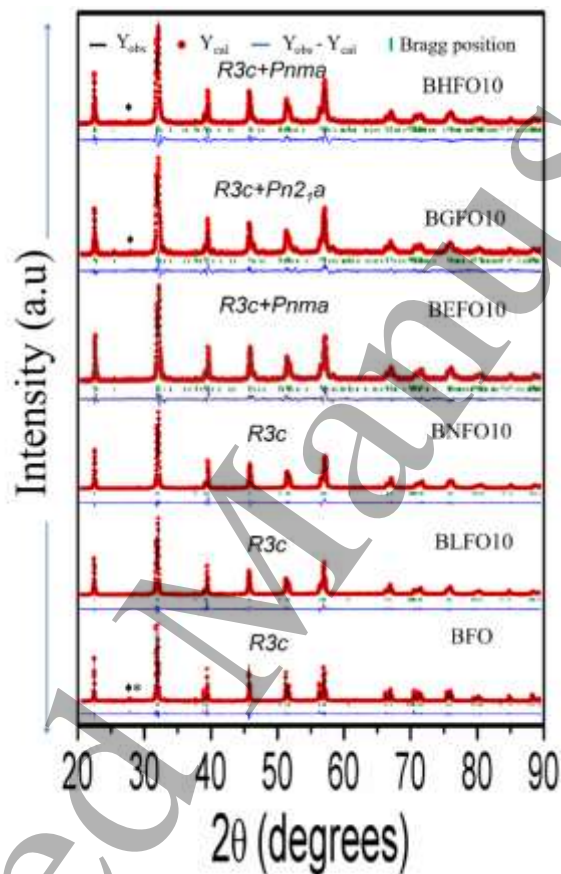
Figure 1. Refined XRD patterns of BFO and BRFO10 compounds. The asterisks ♦ and ∗ represent impurity phases corresponding to $Bi_{25}FeO_{40}$ and $Bi_2Fe_4O_9$, respectively.

Impedance analysis

The frequency variation of real part of impedance (Z') for BFO and BRFO10 compounds between 303 K and 483 K are shown in figure 2. An increase in Z' is observed (for more clarity, see the insets) with the substitution of rare earth element which indicates the improvement in the bulk resistance of the compounds (as Z' is proportional to the resistivity of the compounds) [23].
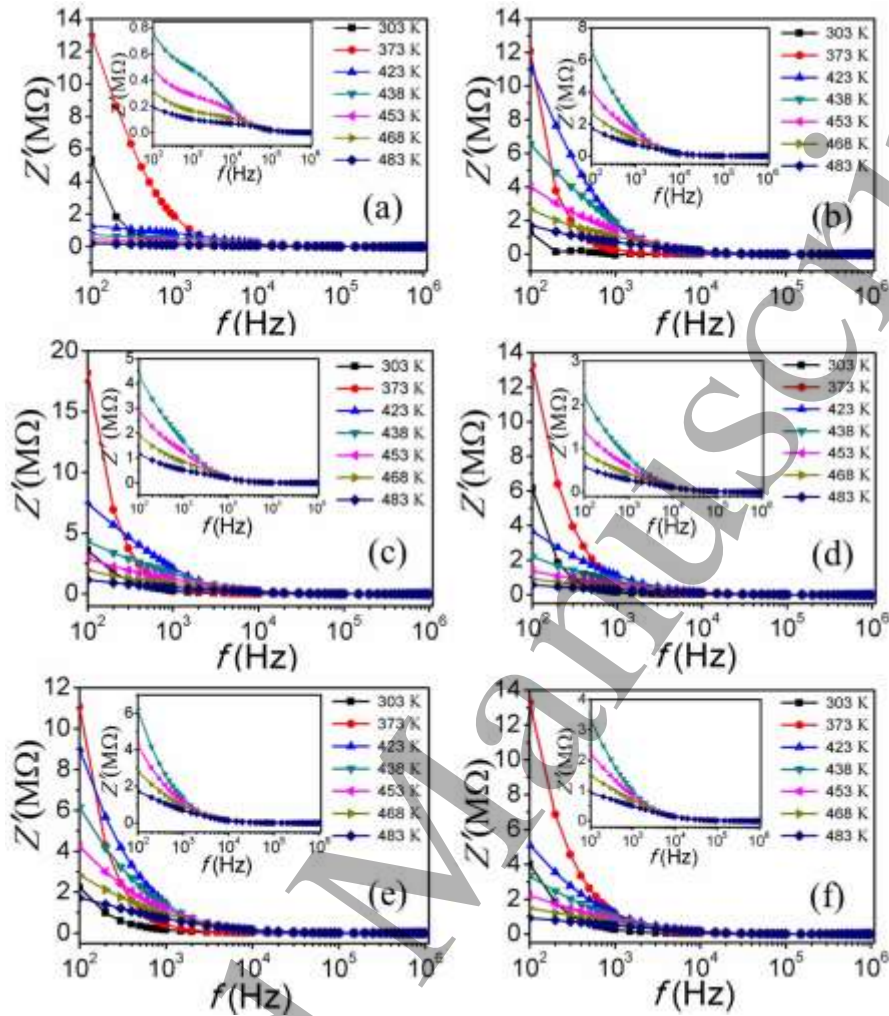
Figure 2. Frequency variation of real part of impedance (Z') for (a) BFO, (b) BLFO10, (c) BNFO10, (d) BEFO10, (e) BGFO10 and (f) BHFO10 compounds. Insets show the frequency variation of Z' from temperature 438 K to 483 K.

The improved Z' is explained as follows. The ionic radii r of Bi^{3+}, La^{3+}, Nd^{3+}, Eu^{3+}, Gd^{3+} and Ho^{3+} ions are 1.17 Å, 1.16 Å , 1.109 Å, 1.066 Å, 1.053 Å and 1.015 Å, respectively. The smaller ionic radius of rare earth ions than the Bi^{3+} ion may create distortions in the crystal structure. The improved insulating character with the rare earth substitution may partly be due to the distortions in the crystal which may increase the height of effective potential barrier for charge carriers [24]. In addition to this, an attempt has been made by us to correlate the improved resistance in BRFO10 compounds with an average bond enthalpy of R-O bonds at A-site. The bond enthalpies of R-O bonds are 799±4 kJ/mol for R = La, 703±13 kJ/mol for R = Nd, 479±10 kJ/mol for R = Eu, 719±10 kJ/mol for R = Gd) and 611±17 kJ/mol for R = Ho, which are greater than that of Bi-O bond (337±12.6 kJ/mol) [25].
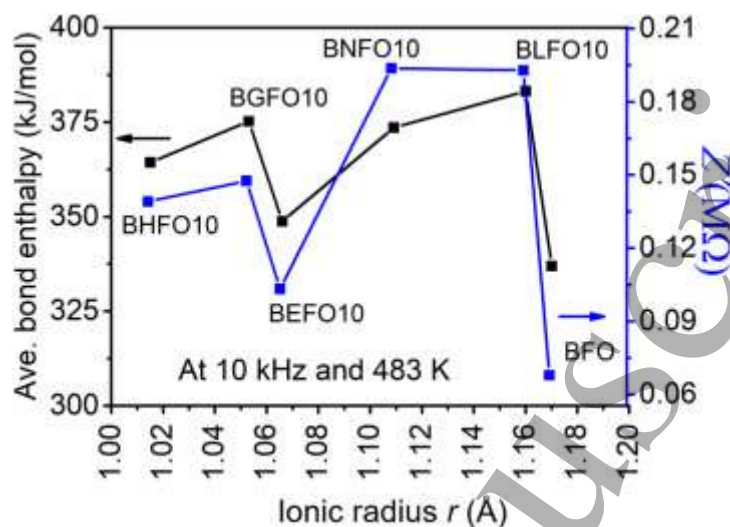
Figure 3. The ionic radius dependence of Z' (at 10 kHz and 483 K) and average bond enthalpy of Bi/R-O bonds for BFO and BRFO10 compounds.

As discussed earlier, the conductivity in the compound directly depends on oxygen vacancies content. The oxygen vacancies are always formed during the synthesis of BFO at high temperature due to the volatilization of Bi^{3+} ions. As bond enthalpy of R-O bonds are stronger than Bi-O bonds, it can be expected that substitution of rare earth elements at Bi site will make the rare earths to form strong bonds with oxygen ions which in turn presumably recovers oxygen vacancies [26] and hence improves the insulating character in BRFO10 compounds.

The ionic radius dependence of Z' (at 10 kHz & at 483 K) and average bond enthalpy of A-site ion (i.e., 90% of Bi-O bond enthalpy and 10% of R-O bond enthalpy) are shown in figure 3. The average bond enthalpy and Z' follow the similar trend with respect to ionic radius r. A similar variations have also been observed at other temperatures (not shown here). It can be inferred from the above mentioned observation that the improved insulating character of BRFO10 compounds strongly depends on the bond enthalpy of R-O bonds.

In order to extract the contributions of grain and grain boundaries to the electrical resistance of the compound, Nyquist plots are considered. Nyquist plots for BFO and BRFO10 compounds from 423 K to 483 K with the temperature interval of 15 K are shown in figure 4. The insulating character of BRFO10 compounds is improved as compared to BFO which can be seen in terms of increase in the intercepts of curves on the Z' axis. The magnitude of intercept is a measure of resistance of the compound. It is observed that the evolution of grain and grain boundary effects

can be observed in the compounds above 423 K. The grain and grain boundary effects are estimated by modelling Nyquist plot with the two equivalent R-C parallel circuit model [16]. The values of grain (/grain boundary) resistance R_g (/R_{gb}), grain (/grain boundary) capacitance C_g (/C_{gb}) and grain (/grain boundary) relaxation time $\tau_{g} = R_g C_g$ (/$\tau_{gb} = R_{gb} C_{gb}$) are extracted for all compounds. Typical values are given in table 1 for all the compounds at temperature 483 K.

Table 1. The typical values of Rgb, Rg, Cgb, C_g, τ_{gb} and τ_{gb} for BFO and BRFO10 compounds at 483 K

Compound	R_{gb} ($M\Omega$)	C_{gb} (nF)	τ_{gb} (mS)	R_g ($M\Omega$)	C_g (pF)	τ_g (μS)
BFO	0.22	2.61	0.57	0.06	45.16	2.71
BLFO10	2.54	1.45	3.68	0.46	42.15	19.39
BNFO10	1.63	2.61	4.25	0.30	45.16	13.55
BEFO10	0.74	7.08	5.24	0.18	266.28	47.93
BGFO10	1.94	0.79	1.53	0.42	110.63	46.46
BHFO10	0.84	2.52	2.13	0.36	202.56	72.92

It is observed that grains offer less resistance than grain boundaries in all compounds at any measured temperature. The temperature variation of grain resistances R_g and grain relaxation times τ_g follow the Arrhenius equations, respectively as given below

$$R_g = R_{og} e^{E_g / k_B T} \tag{1}$$

and

$$\tau_g = \tau_{og} e^{E_{\tau_g} / k_B T} \tag{2}$$

where R_{og} and τ_{og} are constants, E_g and E_{τ_g} are grain conduction and relaxation activation energies, respectively and k_B is Boltzmann constant.
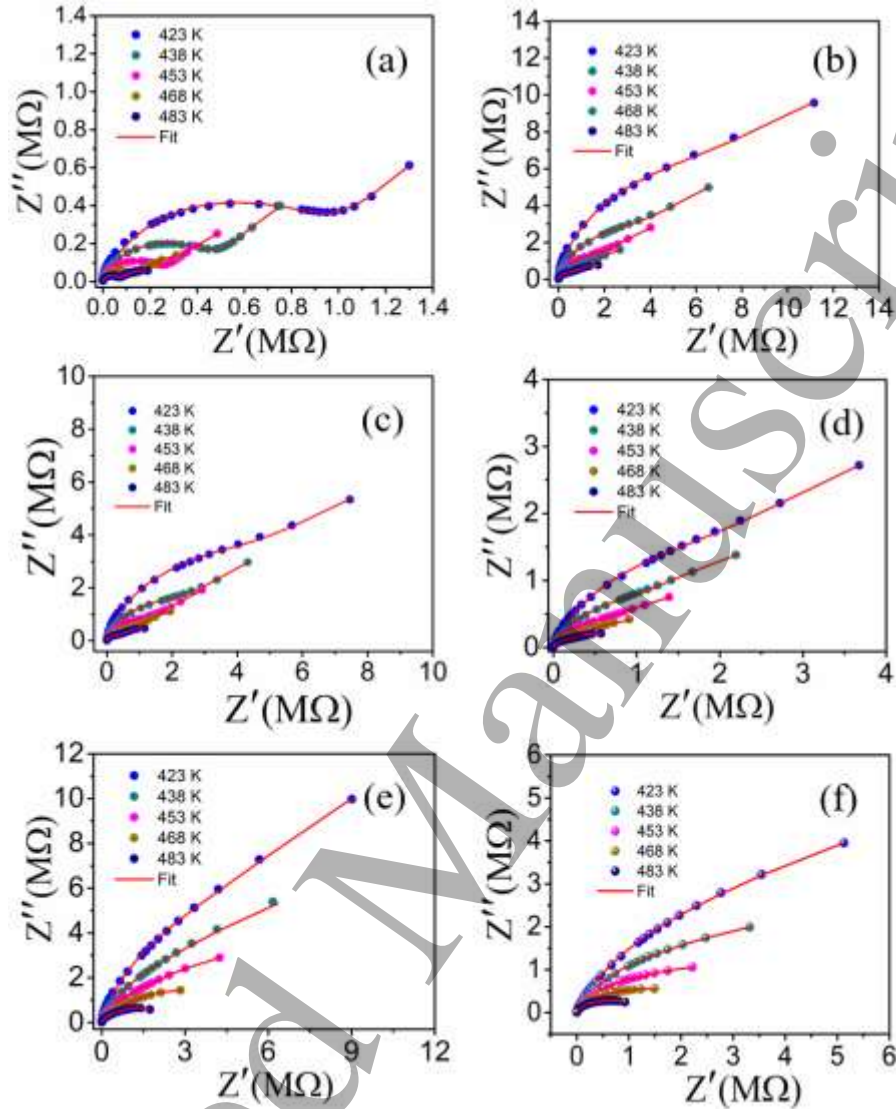
Figure 4. Nyquist plots for (a) BFO, (b) BLFO10, (c) BNFO10, (d) BEFO10, (e) BGFO10 and (f) BHFO10 compounds between the temperatures 423 K to 483 K.

The activation energies E_g and E_{τ_g} are calculated from the linear fitting to the plots drawn between $\ln R_g$ vs $1000/T$ and $\ln \tau_g$ vs $1000/T$, respectively and are shown in figure 5. The obtained values are summarized in table 2. The temperature variation of grain boundary resistances R_{gb} and grain boundary relaxation times τ_{gb} are following Arrhenius equations. The activation energies for grain boundary conduction (E_{gb}) and relaxation time ($E_{\tau_{gb}}$) are calculated from figure 5 (c) and (d) respectively as discussed above. The obtained values are given in table 2.
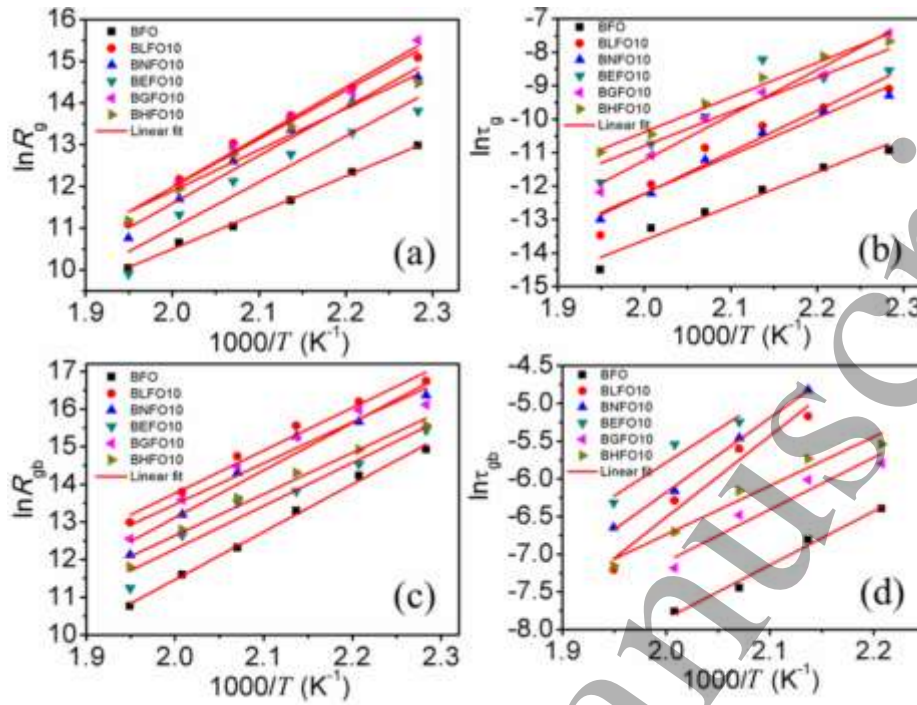
Figure 5. Temperature dependence of (a) grain resistance, (b) grain relaxation times, (c) grain boundary resistance and (d) grain boundary relaxation times for BFO and BRFO10 compounds.

Table 2. Grain, grain boundary resistance and relaxation times activation energies for BFO and BRFO10 compounds.

Compound	E_{R_g}	E_{τ_g}	$E_{R_{gb}}$	$E_{\tau_{gb}}$
BFO	0.75	0.88	1.09	0.61
BLFO10	1.00	1.07	0.98	0.93
BNFO10	0.99	0.98	1.08	0.85
BEFO10	0.95	0.88	0.99	0.76
BGFO10	1.03	1.17	0.94	0.59
BHFO10	0.85	0.90	0.95	0.56

The ionic radius dependence of average bond enthalpies of Bi/R-O bonds and grain resistance R_g (at 483 K) is shown in figure 6. The R_g values for all compounds follows the similar variation as the average bond enthalpies of Bi/R-O bonds varies with r. It indicates that average bond enthalpies play an important role in improving the insulating character of the compound. The variations of grain activation energies E_g with r also show the same dependence as grain resistance

R_g. Hence it can be concluded that the improved insulating character of rare earth substituted compounds depend strongly on bond enthalpies.
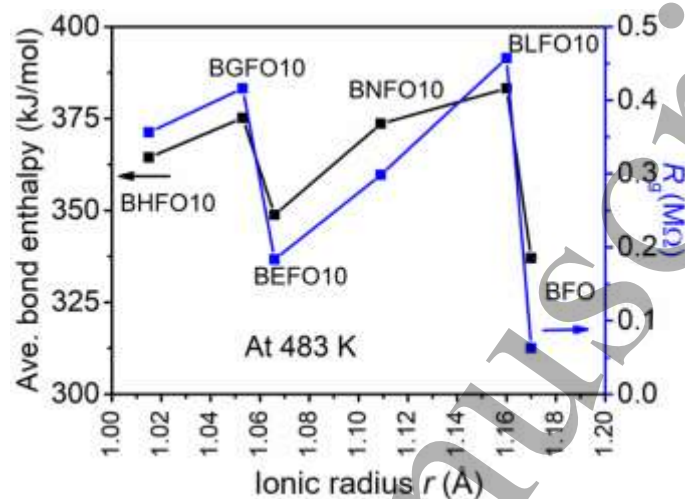
Figure 6. Ionic radius dependence of average bond enthalpies of Bi/R-O bonds and R_g (at 483 K).

Electric modulus studies

Electric modulus studies are conducted because the grain boundary effects are dominated in impedance formalism, whereas grain effects are dominated in electrical modulus formalism. The imaginary part of electric modulus (M'') is calculated using the formula

$$M'' = \omega C_o Z'$$

(3)

The frequency variation of imaginary part of electric modulus (M'') at different temperatures for BFO and BRFO10 compounds is shown in figure 7. The frequency variation of M'' curves are characterized by (i) appearance of peak at unique frequency at a given temperature, (ii) significant broadening in the peak due the presence of distribution of relaxation times (and hence the relaxation is of non-Debye type) and (iii) shift of peak position towards high frequency region with the increase in temperature which indicates the relaxation process is thermally activated [27]. The frequency (f_{max}) corresponding to the maximum of M'' (M''_{max}) follows Arrhenius law

$$f_{max} = f_o e^{-E_M / k_B T}$$

(4)

where f_o is the pre-exponential factor and E_M is the activation energy.
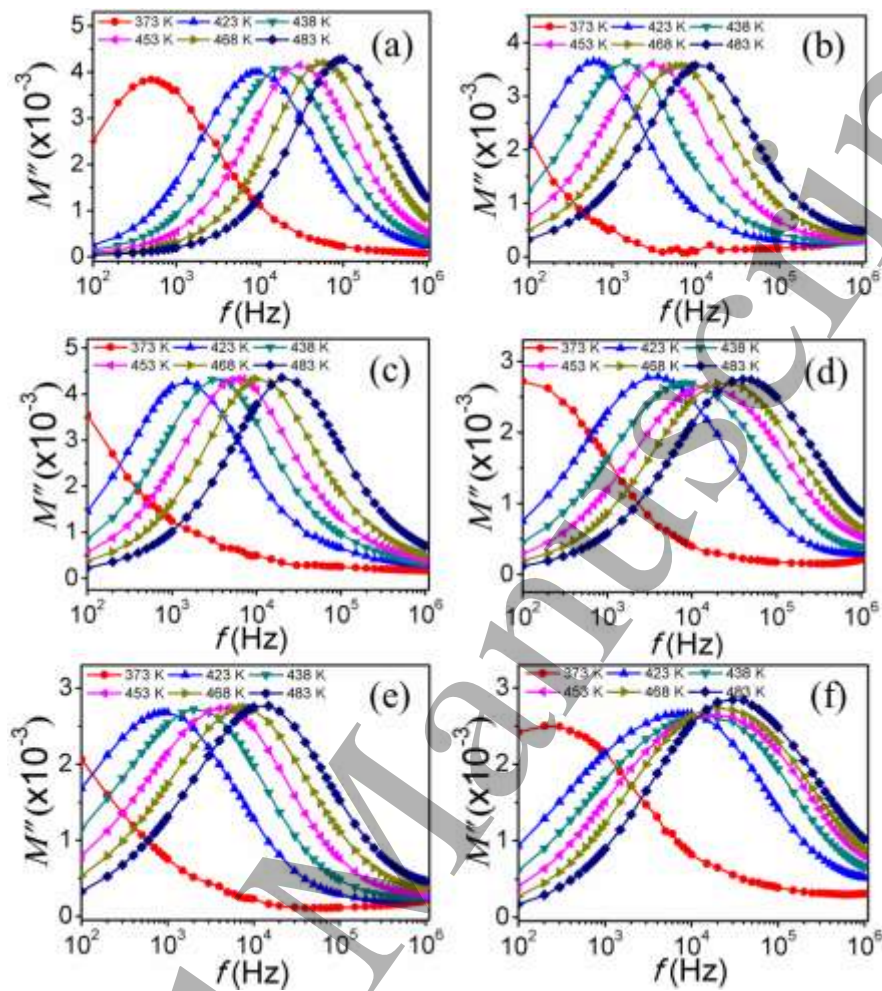
Figure 7. Frequency variation of imaginary part of electric modulus (M'') plots for (a) BFO, (b) BLFO10, (c) BNFO10, (d) BEFO10, (e) BGFO10 and (f) BHFO10 compounds.

The activation energies for BFO and BRFO10 compounds are estimated from linear fit of $\ln(f_{max})$ vs $1000/T$ plots as shown in figure 8 (a). The variation of average bond enthalpy of Bi/R-O bonds and activation energies E_M with r for BFO and BRFO10 compounds are shown in figure 8 (b). It is worth to mention here that the variation of E_M with r follows the similar trend as average bond enthalpies of Bi/R-O bonds varies with r. The aforementioned observation strongly supports the pertinent role of bond enthalpy in improving the insulating character.
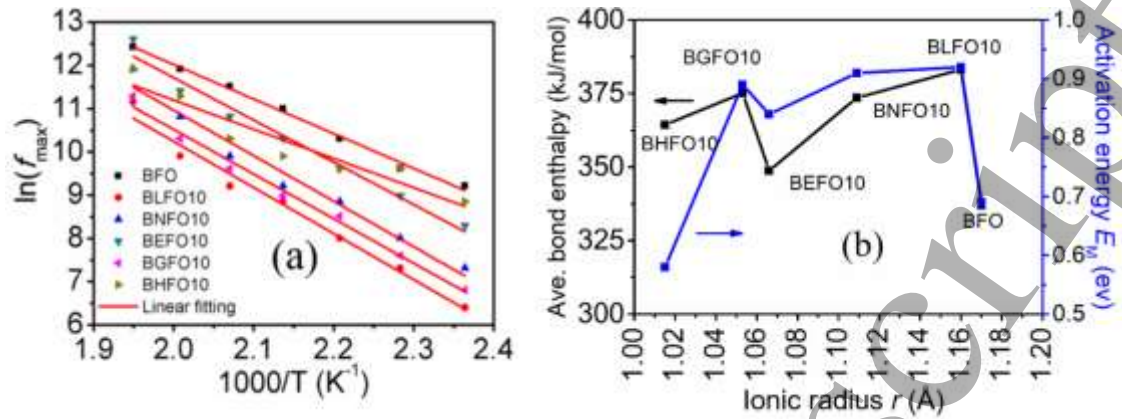
Figure 8. (a) Temperature dependence of $\ln f_{max}$ with $1000/T$, (b) ionic radius dependence of average bond enthalpies of Bi/R-O bonds and activation energies (obtained from M'') for BFO and BRFO10 compounds.

ac conductivity studies

The *ac* electrical conductivity is calculated by using the equation

$$\sigma_{ac} = \varepsilon_o \varepsilon_r \omega \tan \delta \tag{5}$$

where ε_o is the permittivity of free space, ε_r is the dielectric constant, ω is the angular frequency and $\tan \delta$ is the loss tangent.

The frequency dependent *ac* conductivity for BFO and BRFO10 compounds from 423 K to 513 K are observed (not shown here). The typical frequency dependent *ac* conductivity for all compounds at 483 K is shown in figure 9 (a).
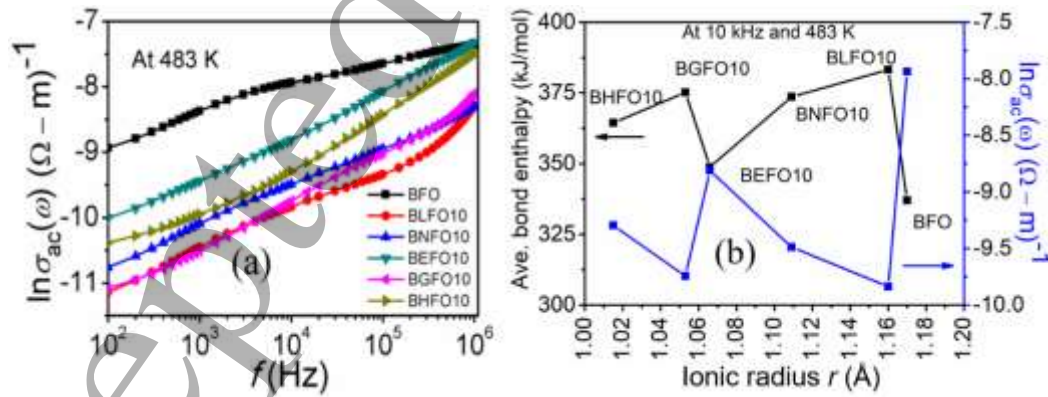
Figure 9. (a) Frequency variation of *ac* conductivity at 483 K, (b) ionic radius dependence of *ac* conductivity (at 483 K and at 10 kHz) and average bond enthalpies of Bi/R-O bonds for all compounds.

It is observed that BFO has the highest conductivity followed by BEFO10, BHFO10, BNFO10, BGFO10 and BLFO10 compounds at any measured frequency and temperature. The variation of *ac* conductivity (at 483 K and at 10 kHz) and average bond enthalpies of Bi/R-O bonds

for all compounds with the ionic radius r is shown in figure 9 (b). The *ac* conductivity behavior with r exactly follows the opposite trend as compared to the variation of average bond enthalpies of Bi/R-O bonds with r. The similar trend has also been observed irrespective of measured temperature range. The important point which can be inferred from the above observations is that "stronger is the bond enthalpy, least is the conductivity in the compound i.e., higher insulating character in it". The same information has also been observed from the impedance and modulus studies. Based on impedance, modulus and conductivity studies, it can be strongly believed that bond enthalpy plays an important role in improving the insulating character of BFO.

It is observed that the activation energies estimated from impedance and modulus formalism are approximately same and match with the activation energy value of long range migrated doubly charged oxide ion vacancies ($V_O^{\bullet\bullet}$) in perovskites [28, 29]. The rather higher value of activation energies in BRFO10 compounds indicates that a reduction in the defect concentration due to the substitution of rare earth elements. The reduction of oxygen vacancies in BRFO10 compounds directly depends on the strength of bond enthalpy of R-O bonds. The reduction in number of oxide ion vacancies causes improved insulating character in BRFO10 compounds. The intensity of dielectric anomaly in the temperature dependence of dielectric data of BFO near 493 K signifies qualitative amount of oxygen vacancies.

Dielectric studies

The temperature dependence of dielectric constant (ε') for BFO and BRFO10 compounds is shown in figure 10. The inset of figure 10 shows the temperature variation of dielectric loss (tanδ). A small dielectric anomaly, which is attributed to the transient interaction between oxygen ions vacancies and Fe^{2+} and Fe^{3+} redox [30], has been observed near 493 K in the dielectric data and the observation is also consistent with the literature [31]. As explained earlier, the oxygen vacancies and Fe^{2+} ions are always created during the formation of the compound during the synthesis of the compounds at high temperature and for longer times. The oxygen vacancies and Fe^{2+} ions are responsible for the conductivity in the compound. BFO exhibits a prominent anomaly indicating presence of relatively more number of oxygen vacancies and Fe^{2+} ions. The partial suppression of anomaly is observed in the case of BHFO10 and BEFO10 compounds indicating suppression of oxygen vacancies due to stronger Ho-O and Eu-O bond enthalpies compared to Bi-O bond enthalpy.
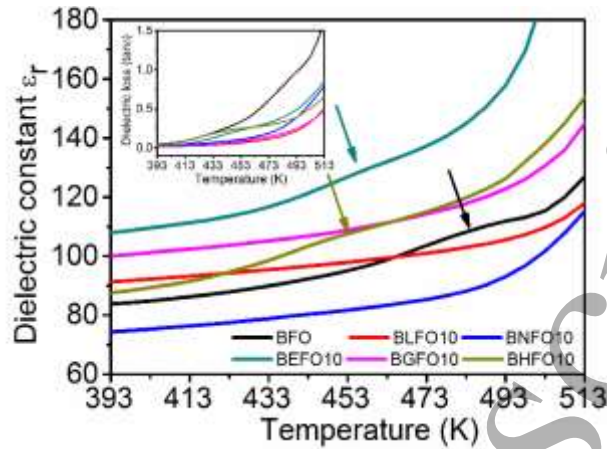
Figure 10. The temperature dependence of dielectric constant (ε') for BFO and BRFO10 compounds. Inset shows the temperature variation of dielectric loss ($\tan\delta$).

The dielectric anomalies in BNFO10, BGFO10 and BLFO10 compounds are almost completely suppressed indicating reduction of large number of oxygen vacancies due to their stronger bond enthalpies. The rare earth element substitution decreases the oxygen vacancies which in turn causes stability of Fe^{2+} / Fe^{3+} couple-oxygen vacancies interactions.

Conclusions

BFO and $Bi_{0.90}R_{0.10}FeO_3$ [BRFO10, R = La (BLFO10), Nd (BNFO10), Eu (BEFO10), Gd (BGFO10) and Ho (BHFO10)] compounds were synthesized by conventional solid-state reaction. The grain and grain boundary resistances were improved and *ac* conductivity was reduced due to decreased oxygen vacancies in the substituted compounds. Stronger bond enthalpy of R-O bonds led to the great reduction of oxygen vacancies in BRFO10 compounds and hence the greater insulating character in them. In other words, a strong correlation was found between the insulating character of $Bi_{0.90}R_{0.10}FeO_3$ compounds and the bond enthalpy of R-O bonds. The impedance and *ac* conductivity clearly indicated that bond enthalpy played an important role in tuning the insulating character of BFO. The intensity of dielectric anomaly around 493 K in BFO and BRFO10 clearly demonstrated qualitatively the oxygen vacancies content in the compounds which was in consistence with bond enthalpy concept. This study will be of great interest to the research community to understand the potential of the rare earth substituent in tuning the insulating character of $BiFeO_3$.

Acknowledgements

References

1   Sosnowska I, Peterlin-Neumaier T, Steichele E 1982 J. Phys. C: Solid State Phys. **15** 4835
2   Hill N A 2000 J. Phys. Chem. B **104** 6694
3   Catalan G, Sardar K, Church N S, Scott J F, Harrison R J, Redfern S A T 2009 Phys. Rev. B **79** 212415
4   Ramesh R and Spaldin N A 2007 Nat. Mater. **6** 21
5   Nari Jeon, Dibyaranjan Rout, Ill Won Kim and Suk-Joong L. Kang 2011 Appl. Phys. Lett. **98** 072901
6   Catalan G, Scott J F 2009 Adv. Mater. **21** 2463
7   Hu W W, Chen Y, Yuan H M, Li G G, Qiao Y, Qin Y Y, and Feng S 2011 J. Phys. Chem. C **115** 8869
8   Rao T D, Asthana S 2012 J. Appl. Phys, **116** 164102.
9   Li J B, Rao G H, Xiao Y, Liang, J K, Luo J, Liu G Y, Chen J R 2010 Acta Mater. **58** 3701
10 Chang W S, Tu C S, Chen P Y, Chen C S, Lin C Y, Feng K C, Hsieh Y L, Y. Huang Y H 2017 J. Alloys Compds **710** 670-679.
11 Singh H, Yadav K L 2015 J. Phys. D: Appl. Phys. **48** 205001,
12 Qian F Z, Jiang J S, Guo S Z, Jiang D M, Zhang W G 2009 J. Appl. Phys. **106** 084312.
13 Samita P, Parida B N, Das P R, Choudhary R N P 2013 Appl Phys A **112** 387–395
14 Mukherjee A, Basu S, Manna P K, Yusuf S M, Pal M 2014 J. Alloys Compds. **598**, 142
15 Shivanand M, Swarup K, Rajasekhar B and Varma K B R 2016 Mater. Res. Express **3,** 065009
16 Rao T D, Ranjith R, and Asthana S 2014 J. Appl. Phys. **115**, 124110
17 Rao T D, Karthik T, Srinivas A, Asthana S, 2012 Solid State Commun, **152** 2071–2077.
18 Rao T D, Karthik T, Srinivas A, Asthana S, AIP Conf. Proc. 1536 (2013), 1007,
19 Madolappa S, Kundu S, Bhimireddi R and Varma K B R 2016 Mater. Res. Express **3** 065009
20 Uniyal P and Yadav K L 2008 Mater. Lett. **62**, 2858
21 Rao T D, Karthik T, and Asthana S 2013 J Rare Earths **31 No. 4**, 370
22 Rao T D, Kumari A, Niranjan M K, Asthana S 2014 Physica B **448**, 267
23 Tiwari B and Choudhary R N P 2010 J. Alloys Compds. **493**, 1
24 Mukherjee A, Basu S, Chakraborty G, Pal M 2012 J. Appl. Phys. **112** 014321.
25 Kerr J A, CRC Handbook of Chemistry and Physics, 81st ed. (CRC Press, Boca Raton, Florida, USA, 2000).
26 Indrani C, Neeraj P, Bdikin I, Puli V S, Katiyar R S and Kholkin A L 2012 J. Phys. D: Appl. Phys. **45**, 055302
27 Mishra A, Choudhary S N, Choudhary R N P, Murthy V R K, Kamal P 2012 J. Mater Sci: Mater Electron., **23(1)**, 185
28 Cordero F, Ferretti M, Cimberle M R, Masini R 2003 Phys. Rev. B **67**, 144519
29 Srivastava A, Garg A, and Morrison F D 2009 J. Appl. Phys. **105**, 054103
30 Mishra R K, Pradhan D K, Choudhary R N P, Banerjee A 2008 J. Phys.: Condens. Matter **20**, 045218
31 Reetu R, Agarwal A, Sanghi S and Ashima A 2011 J.Appl.Phys. **110**, 073909